

# ASTOS Orbit Generator – Rapid Creation of Quasi-Optimal Orbital Transfers in the CR3BP

Maximilian Walther <sup>(1)</sup>, Andreas Wiegand <sup>(2)</sup>

<sup>(1)</sup> *Astos Solutions GmbH, Meitnerstr. 8, 70563 Stuttgart, maximilian.walther@astos.de*

<sup>(2)</sup> *Astos Solutions GmbH, Meitnerstr. 8, 70563 Stuttgart, +49-711-892633-10,  
andreas.wiegand@astos.de*

## ABSTRACT

The Orbit Generator Tool, part of the ASTOS software, rapidly creates and simulates quasi-optimal solutions for orbital transfers in the circular Earth-Moon system and to libration point orbits. Mission designers can select impulsive or low-thrust propulsion systems, short- or long-time transfers, and more complex trajectory arcs employing e.g. fly-bys or manifolds. Different algorithms are used to compute the transfers, including a multiple-shooting differential corrections method for impulsive transfers and a modified version of Petropoulos' Q-Law for low-thrust transfers. Each transfer is subdivided into different phases, and the tool optimizes the characteristic parameters of each section to output the most fuel- or time-efficient trajectories. By employing the MIDACO optimizer, a front of Pareto-optimal solutions can be created and then be used to evaluate the trade-off of those performance measures. The import of selected trajectories into ASTOS scenarios for further optimization and mission analysis is supported.

This paper outlines the tool's architecture, algorithms, and reference solutions in the CR3BP system. The optimized trajectories are compared with solutions from literature and found to be at least competitive if not favorable. Finally, an outlook into future developments, such as the implementation of the bicircular restricted four-body problem and the transformation into high-fidelity ephemeris, is given.

## 1 INTRODUCTION

The interest in the Moon as a target for scientific, explorational, and commercial space missions has been rising in the past years. In 2022 alone, (at least) eight missions to the Moon were launched [1] and this number can be expected to increase in the near future. NASA's ARTEMIS program will lay the foundation for frequent travel across cislunar space. Just the construction and operation of the Gateway, which is planned to be placed in a near-rectilinear halo orbit (NRHO) around the libration point  $L_2$ , will require several missions with different profiles: Manned flights have a higher emphasis on getting to the Gateway quickly, so as not to spend too much time in the Van Allen belts, while cargo missions may prioritize savings in propellant, in order to deliver as much mass as possible to their destination and therefore choose electrical propulsion systems.

The design of transfer trajectories in cislunar space is however not trivial. Transferring spacecraft into their target orbits as efficiently as possible enables greater payload masses or operational lifetime for their missions. In the design process, however, mission planners require a good overview of various trajectory possibilities before moving on to in-depth optimization and analyses. Especially for missions with differing requirements, there is no "one-fits-all" approach. The ASTOS Orbit Generator Tool offers a rapid and flexible way of creating trajectories for

transfers in cislunar space. Instead of focusing on the optimization of single transfer types, the tool allows to draw up transfers between several types of orbits in the circular restricted three-body problem (CR3BP). This includes Keplerian orbits around Earth, low lunar orbits (LLOs), Lagrangian point orbits (halos) or distant retrograde orbits (DROs). To enable trade-offs between transfer duration and required propellant mass, the transfers can be computed both for continuous low-thrust and impulsive approaches. Furthermore, even with a selected propulsion system a multi-objective optimization is performed to allow the selection of a transfer which best fulfils propellant or temporal requirements. After selecting one solution for further analysis, the tool loads the trajectory into an ASTOS scenario for further optimization and mission analysis tasks.

This work outlines the architecture of the Orbit Generator Tool, gives an insight into the algorithms used, and aims to highlight the tool’s capabilities by comparing obtained trajectories to results from literature.

## 2 THEORETICAL BACKGROUND

This chapter presents the dynamical system in which the transfer trajectories are computed. In addition to the description of governing differential equations, the dynamic properties which entail periodic solutions and paths to/from these solutions – namely manifolds – are also highlighted.

### 2.1 Circular Restricted Three-Body Problem

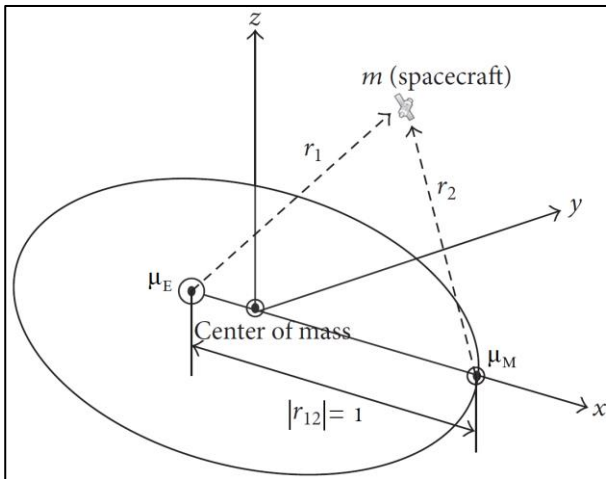
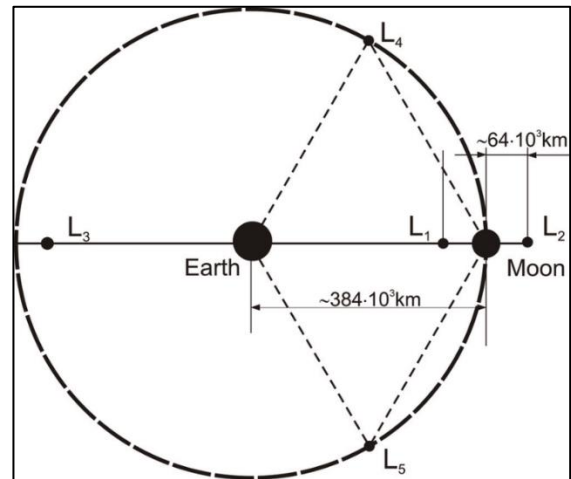


Figure 2-1: (a) CR3BP Coordinate System [2]



(b) Positions of the Earth-Moon Libration Points (not to scale) [3]

#### Definition, Coordinate System, Normalization

The circular restricted three-body problem not only includes a useful coordinate system to express and compute cislunar trajectories, but also models the simplified circular motion of the primary with gravitational parameter  $\mu_E$  (i.e. the Earth) and the secondary with gravitational parameter  $\mu_M$  (i.e. the Moon) around their common barycenter. The system is defined by the parameter  $\mu$ , which expresses the ratio of the Moon’s mass to the total system mass, as stated in Eq. (1).

$$\mu = \frac{\mu_M}{\mu_E + \mu_M} \quad (1)$$

The CR3BP’s origin lies in the Earth-Moon barycenter and the system is rotating with the constant angular velocity  $\omega_{E-M}$ , which is defined in Eq. (2).

$$\omega_{E-M} = \sqrt{\frac{\mu_E + \mu_M}{a_M^3}}, \quad (2)$$

where  $a_M$  is the semi-major axis of the circular orbit of the Moon around the Earth. Therefore, both celestial bodies' positions are constant in CR3BP coordinates and are defined to lie on the  $x$ -axis. The  $z$ -axis points in the direction of the angular velocity of the system and the  $y$ -axis completes the right-hand system (see Figure 2-1 (a)).

Moreover, the CR3BP is commonly nondimensionalized using  $a_M$  as length unit (LU) and  $\omega_{M-E}^{-1}$  as time unit (TU). Consequently, the distance between Earth and Moon becomes 1.0 and their positions are  $\mathbf{r}_E = [-\mu \ 0 \ 0]^T$  and  $\mathbf{r}_M = [1 - \mu \ 0 \ 0]^T$ . The system-defining variables are given in Table 1. The values of the gravitational parameters are adapted according to [4], the angular velocity is taken from the Astronomical Almanac [5], and the distance of Earth and Moon is adjusted accordingly to Eq. (2).

Table 1: CR3BP System-Defining Parameters

Parameter	Value	Unit	Dimensionless Value
$\mu_E$ – Grav. Parameter of the Earth	398600.435507	$km^3s^{-2}$	0.98784941560529029
$\mu_M$ – Grav. Parameter of the Moon	4902.800118	$km^3s^{-2}$	0.01215058439470971
$a_M$ – Distance of Earth and Moon	384747.2177751845	$km$	1.0
$\omega_{E-M}$ – Angular Velocity of System	0.22997150177512	$day^{-1}$	1.0

### State, Equations of Motion

The spacecraft state  $x$  in the CR3BP is defined by its position  $\mathbf{r}$ , velocity  $\mathbf{v}$  and mass  $m$ :

$$\mathbf{r} = [x \ y \ z]^T, \mathbf{v} = [\dot{x} \ \dot{y} \ \dot{z}]^T, \mathbf{x} = [\mathbf{r}^T \ \mathbf{v}^T \ m]^T \quad (3)$$

The position is expressed with respect to the system's barycenter. With the primary and secondary celestial bodies' positions  $\mathbf{r}_E$  and  $\mathbf{r}_M$  the spacecraft's relative position to the Earth  $\mathbf{r}_1$  and the Moon  $\mathbf{r}_2$  result to:

$$\mathbf{r}_1 = [x + \mu \ y \ z]^T, \mathbf{r}_2 = [x - (1 - \mu) \ y \ z]^T \quad (4)$$

The description of the unperturbed CR3BP system dynamics (i.e., without thrust accelerations) benefits from the definition of the pseudo-potential  $U$ , as provided in Eq. (5).

$$U = \frac{1}{2}(x^2 + y^2) + \frac{1 - \mu}{\|\mathbf{r}_1\|} + \frac{\mu}{\|\mathbf{r}_2\|} \quad (5)$$

For the original derivation of the pseudo-potential, please refer to [6]. When adding thrust acceleration into the system, the equations of motion take the form shown in Eq. (6).

$$\begin{aligned} \ddot{x} - 2\dot{y} &= \frac{\partial U}{\partial x} + f_x(t) \\ \ddot{y} + 2\dot{x} &= \frac{\partial U}{\partial y} + f_y(t) \\ \ddot{z} &= \frac{\partial U}{\partial z} + f_z(t) \\ \dot{m} &= -\frac{F(t)}{c_e} \end{aligned} \quad (6)$$

where  $f_x$ ,  $f_y$  and  $f_z$  represent the components of the nondimensionalized thrust acceleration  $\mathbf{f}$ . An additional differential equation is added to govern the change in spacecraft mass, whenever a thruster is active. Here,  $F$  is the nondimensionalized thrust magnitude and  $c_e$  the nondimensionalized effective exhaust velocity of the propulsion system.

In case of impulsive transfers, the thrust is set to zero and maneuvers are implemented by adding instantaneous changes in velocity  $\Delta v$  to the state. The change in mass  $\Delta m$  is then modelled by Tsiolkovsky's rocket equation.

## 2.2 CR3BP Periodic Solutions

In the CR3BP, five libration points arise in which the gravitational and fictitious (i.e., centrifugal and Coriolis) accelerations cancel out. A spacecraft placed in any of these points will remain there and rotate along with the system. As can be seen in Figure 2-1 (b), all five Lagrangian points – as they are also called – lie in the  $xy$ -plane of the system.

For the application, special attention is given to the near-lunar collinear Lagrangian points  $L_1$  and  $L_2$ , because their unstable equilibrium enables periodic solutions. Spacecraft can be placed in such libration orbits to orbit about  $L_1/L_2$  rather than about the Moon itself.

The periodic solutions considered for the Orbit Generator Tool are the so-called halo orbits, which can be split into two families – southern and northern. After specifying the reference point ( $L_1$  or  $L_2$ ) and selecting the desired family, a specific halo orbit can be identified through parameters like its out-of-plane amplitude  $A_z$ , its period, its stability, or its periselenium distance. The northern and southern families of NRHOs around  $L_1$  and  $L_2$  are depicted in Figure 2-2 (a).

In addition, the Orbit Generator Tool allows the calculation of another type of periodic solutions – the so-called distant retrograde orbits. These do not orbit a single Lagrange point but the Moon at a very high altitude and in the opposite direction of the lunar orbit around the Earth, which explains the name. The family of DROs is depicted in Figure 2-2 (b). An individual member of the family can be uniquely identified by its orbital period.

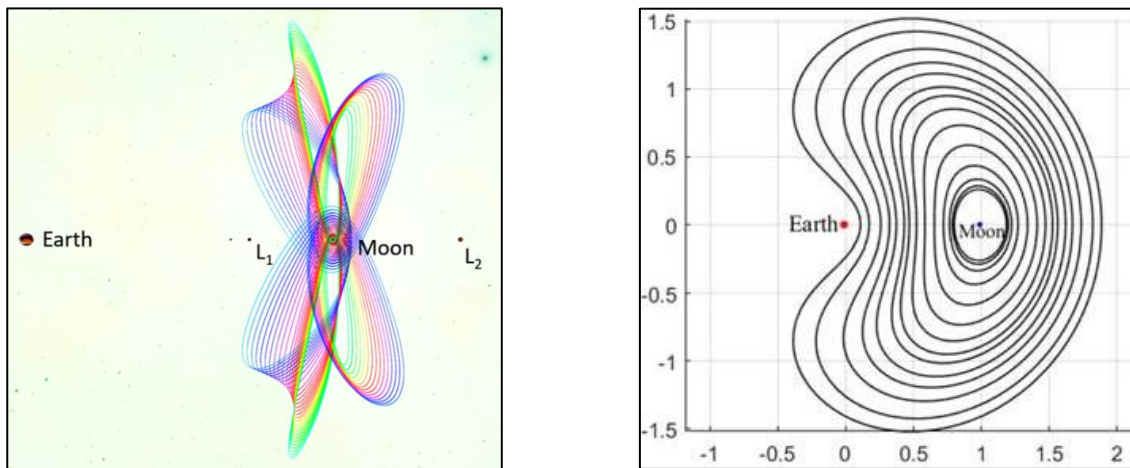


Figure 2-2: (a) Northern/Southern NRHO Families [7]

(b) DRO Family [8]

The periodic solutions are computed by first utilizing Richardson's approximation as an initial guess [9] and then correcting the initial guess using Howell's differential corrections algorithm [10]. Finally, the desired solution is found by employing continuation schemes [11] to step through the members of the orbit family until the parameters match. To reduce the time necessary to find the desired solution, a database containing a multitude of halo and DRO initial states is built. For more detailed explanations on the process of generating periodic solutions the reader is referred to [12].

### 3 TRANSFER STRATEGIES

In the Orbit Generator Tool, each orbital transfer is subdivided into a number of phases, which act as building blocks of the trajectory. Each phase is characterized by the spacecraft's behavior or the trajectory it follows and can be uniquely defined through a set of parameter values. In the following, the different phases to compile an orbit transfer, their parametric characteristics and algorithmic concepts are explained.

#### 3.1 Initial and Target Orbits

In order to define a transfer, the departure and destination orbits must be established. The available options are Keplerian orbits around either Earth or Moon, halo orbits around the libration points of the system, or DROs. While the general type of orbit and its dimensions must be fixed, the exact point of departure or arrival and the orbit's spatial orientation (in the case of Keplerian orbits) can be left open for optimization.

In detail this means for **Keplerian orbits** that the semi-major axis  $a$  and the eccentricity  $e$  have to be defined during the set-up of the transfer. The other classical orbital elements, such as inclination  $i$ , argument of periapsis  $\omega$ , right ascension of the ascending node  $\Omega$  (RAAN) and true anomaly  $\theta$  can be either fixed or left open for optimization, as desired. This allows for flexible or strict definition of the orbit.

For **halo orbits** and **DROs**, the member of the respective family must first be selected uniquely. As already mentioned in section 2.2, this can be done by specifying a parameter like the ( $x/y/z$ )-amplitude, orbital period, distance of the apo-/periselenium, the Jacobi constant or the stability index. The exact point at which the spacecraft will arrive/depart at the desired orbit, however, can again be left to the optimizer. This is governed via a non-dimensional parameter whose value indicates how far along one revolution the desired point is. The value 0 corresponds to the crossing of the  $xz$ -plane in positive  $y$ -direction. Along one orbit, the value increases steadily until it reaches 1 when the starting point is reached again.

#### 3.2 Intermediate Trajectory Arcs with Impulsive Transfers

After having defined the transfer's starting point and destination, the intermediate trajectory arcs connecting the initial and target orbit must be chosen. In the case of impulsive transfers, changes of velocity  $\Delta v$  are allowed at each border between phases, while during each phase only coasting is possible. For the determination of the magnitude and direction of these impulsive  $\Delta v$ , the so-called Lambert arc becomes the central element.

A **Lambert arc** is the resulting trajectory, coming out of the solution to Lambert's problem, in which two positions in space must be connected by a coasting arc of a certain duration. Given two states and a time-of-flight (TOF), a Lambert arc to connect their positions can be computed and two  $\Delta v$  (one at departure and one at arrival) are then derived. By optimizing the TOF, which is the only parameter used for Lambert arcs, the required  $\Delta v$  and therefore propellant mass can be reduced. While Lambert's problem has an analytic solution in the two-body problem (2BP) with just one central body, in the CR3BP it requires numerical approaches. The Orbit Generator Tool employs an iterative corrections approach as sketched out in [13]. However, to achieve higher convergence rates in the – at times chaotic and sensitive – CR3BP a multiple shooting approach was implemented. For more information, please refer to [14] and [15].

When departing from or targeting halo orbits, the dynamic properties of the CR3BP can be exploited by making use of the so-called **invariant manifolds**. These structures utilize the (in-)stability properties of halo orbits to make coast arcs that lead towards/away from these orbits requiring a negligible amount of propellant. This enables a spacecraft to cheaply navigate through the Moon's sphere of influence. They are created by perturbing the state on a halo by a small amount in the direction of the (un-)stable eigenvector of the monodromy matrix [10] and then

propagating forwards/backwards in time. Sets of invariant manifolds are visualized for a libration orbit in Figure 3-1. Given the state on a halo to depart from/arrive at, the exact shape of the manifold is determined by the magnitude of the perturbation and then for how long the spacecraft shall follow it. Additionally to those two parameters, the Orbit Generator Tool allows for an additional impulsive  $\Delta v$  vector, increasing the total number of parameters associated with manifolds to five. It is up to the user how many of those are fixed or left open to optimization.

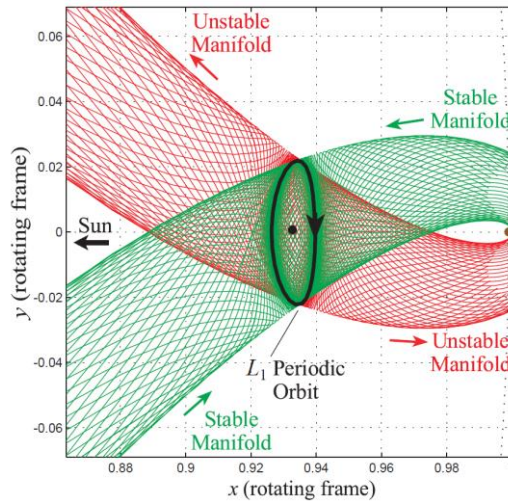


Figure 3-1: Stable and Unstable Manifolds of a Sun-Earth Libration Orbit [16]

The Orbit Generator Tool furthermore allows to add **fly-by points** to a transfer. More specifically, a position near the Moon at which an impulsive  $\Delta v$  maneuver is to be flown can be specified. It is then connected via two Lambert arcs to the preceding and successive phases. The magnitude and direction of  $\Delta v$  is determined completely implicitly by those arcs. The user can however specify or optimize the position of the fly-by point in selenocentric polar coordinates.

### 3.3 Intermediate Trajectory Arcs with Low-Thrust

For transfers using continuous or intermittent low-thrust, the previously presented approaches using impulsive  $\Delta v$  maneuvers are not applicable. For this reason, no Lambert arcs or fly-by points can be defined for these kinds of trajectories. In order to still be able to design transfers from one orbit into another, a control law to determine necessary thrust directions for any state along the transfer is employed.

To be more precise, for **low-thrust phases** the tool uses an adapted version of the so-called **Q-Law**, which in its original form was first published by Petropoulos [17] and then refined in the following years [18, 19]. It uses a Lyapunov function  $Q$  to analytically determine the thrust direction for transfers into Keplerian orbits. Thereby, it can guide an electrically propelled spacecraft into target orbits, matching up to five of the orbital elements to their respectively desired values:  $a$ ,  $e$ ,  $i$ ,  $\omega$  and  $\Omega$ . The Q-Law is, however, not able to predetermine the duration of the transfer or to target arrival at a specific true anomaly  $\theta$  on the destination orbit. Furthermore, since only Keplerian orbits can be targeted, no halo-to-halo low-thrust transfers are currently possible.

Transfers originating from a Keplerian orbit but targeting a halo orbit are still covered by the Q-Law algorithm, though. This is enabled through backwards propagation, in which the Q-Law is still functional by inverting the thrust direction: In those cases, propagation starts at the target orbit and the spacecraft is guided backwards through time by the Q-Law to arrive at its parking orbit.

The same idea is also used for computing transfers from a geocentric Keplerian orbit into a selenocentric orbit (LLO): Although, the Q-Law was originally developed for the use within an unperturbed two-body problem (2BP), it can still be applied in the 3BP, as long as the gravitational perturbation of the third body does not become too large. The Q-Law has demonstrated good

convergence rates, as long as it is operated within the sphere of influence (SOI) of the relevant celestial body, i.e., for LLOs it works within the Moon's SOI, whose radius is commonly approximated (see [20]) as expressed in Eq. (7):

$$r_{SOI} = a_M * \left( \frac{\mu_M}{\mu_E} \right)^{0.4} \quad (7)$$

Since for the description of Keplerian orbits in a transfer from Earth to LLO (or vice versa) the reference system must be switched, two separate Q-Law phases must be used – one geocentric and one selenocentric. They are connected at a so-called **patch point**, which lies on the border of the Moon's SOI. Starting from this patch point, both Q-Law phases are propagated, one of which backwards in time. This is sketched in Figure 3-2.

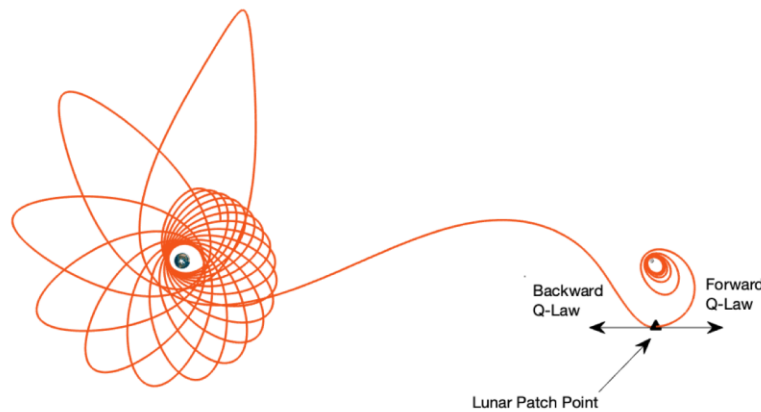


Figure 3-2: Schematic Drawing of the Propagation Principle for Low-Thrust Transfers from Geocentric to Selenocentric Keplerian Orbits [21]

The Q-Law algorithm in the Orbit Generator Tool contains some adaptations compared to its original formulation. First, the introduction of an effectivity value allows for intermediate coasting. The thrust is shut-off whenever the effectivity drops below a certain (optimizable) threshold. The higher the threshold, the more often coasting phases can be expected, which increases the TOF but decreases the required propellant mass, because the thrusters are utilized in more efficient locations only. Second, in order to avoid on-off jitter, once the thrust has been shut-off, it stays off for some amount of time, which the user can specify. For improved final convergence into the target orbit, a dead band as suggested by Lantukh [22] was implemented. Further adaptations like considering eclipse phases or improving the computational efficiency by avoiding strongly changing thrust direction from one time step to another are explained in [12].

The performance of the Q-Law depends on the choice of the weighting factors associated with each of the targeted orbital elements and the effectivity threshold mentioned previously. These constitute the optimizable parameters for low-thrust phases. Generally, it can be said, that a higher weighting factor for a certain element increases its priority in the computation of the thrust strategy. This means that usually, this element will converge to its target value faster, for which it may accept increased deviations in the other orbital elements in the meantime. The interdependence of the elements makes a good initial guess for the weighting factors difficult, but the optimizer is usually able to quickly find improvements by adjusting their values.

In case the definition of a patch point becomes necessary to connect two Q-Law phases, its state definition is included into the optimization problem. As it lies on the Moon's SOI, this definition comprises five optimizable parameters: two angles describing its position on the sphere and three velocity components in  $x$ -,  $y$ - and  $z$ -direction.

Like impulsive cislunar transfers, in low-thrust transfers **manifolds** are also used to approach and depart halo orbits and DROs. Their positioning and length are again determined by optimizable

parameters governing the point of reference on the periodic orbit and the coast duration along the manifold. Since with low-thrust propulsion systems no impulsive change in velocity can be assumed, though, the perturbation, which is necessary to create manifolds, is instead approximated by a **low-thrust perturbation phase**. During this phase, thrust is applied in the direction of the velocity component of the (un-)stable eigenvectors. The magnitude of the perturbation is therefore governed by the duration of perturbation phase.

## 4 SET-UP OF THE TOOL

The Orbit Generator Tool allows to configure the scenario, initial and final orbit, as well as initial guesses and bounds for the optimizable parameters associated with the chosen transfer phases. Moreover, the optimizer settings can be made and finally, the optimization log output is printed. This chapter outlines the workflow for setting up the optimization of a desired transfer in the Orbit Generator Tool.

### 4.1 Scenario Definition

Upon opening the Orbit Generator Tool, the first set-up tab is displayed. It is used to configure the general settings and environment in which the transfer shall take place. This includes the selection of the dynamic system (Earth or Earth-Moon<sup>1</sup>), the type of transfer maneuvers (impulsive or low-thrust) and a reference Julian date at which the transfer shall take place. Constraints to the acceptable solutions are defined next. Besides the maximum transfer duration, this entails the maximum  $\Delta v$  for impulsive transfers and the maximum expended propellant mass for low-thrust transfers. For impulsive transfers, it can be decided whether a fly-by shall take place by setting the corresponding field to *Enabled* or *Disabled*. For low-thrust transfers however, the user must provide information about system masses and the thruster's capabilities, i.e., its thrust  $F$  and effective exhaust velocity  $c_e$ . As already mentioned in section 3.3, a minimum time until the thruster may be activated again after shutting off must also be defined to avoid on-off jitter. Two examples for the set-up of the *Scenario* tab are shown in Figure 4-1.

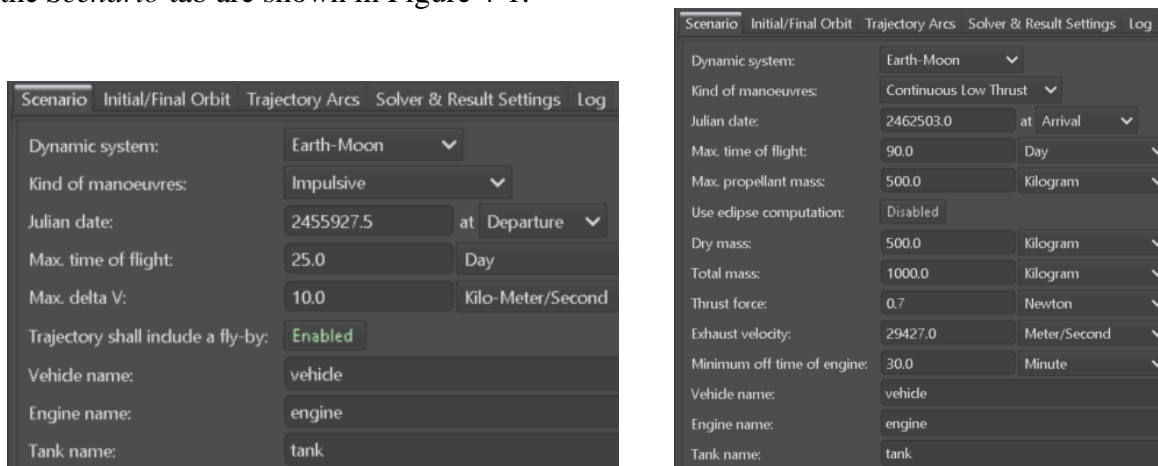


Figure 4-1: Scenario Settings for (a) Impulsive Transfer (b) Low-Thrust Transfer

### 4.2 Initial and Final Orbit Settings

In the second tab, the initial and final orbit are defined. Currently, three types of orbits are available for selection: Keplerian orbits, Lagrangian point orbits and DROs. Their set-up is straightforward.

<sup>1</sup> The integration of the Sun-Earth-Moon bi-circular restricted four-body problem (BCR4BP) is currently in development. The capability of computing transfers in this system has been demonstrated in [32].

Beside the definition of the general type of orbit, a reference body and if applicable, the affiliation to a certain family, it simply requires the specification of a characteristic parameter. In the case of Keplerian orbits, the major semi-axis and eccentricity must be specified instead. In case a manifold shall be used to depart from/arrive at a halo or DRO, the corresponding field must be set to *Enabled*. Two examples for the set-up of the *Initial/Final Orbits* tab are shown in Figure 4-2.

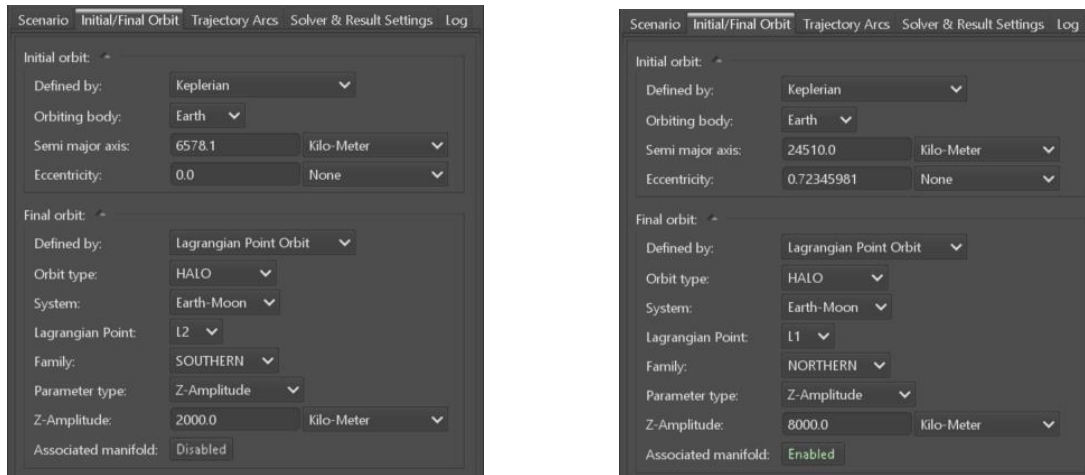


Figure 4-2: Orbit Settings for (a) Transfer from LEO to L2 Halo (b) Transfer from GTO to L1 Halo

### 4.3 Trajectory Arc Parameters

In the *Trajectory Arcs* tab, the parameters of each phase are defined and their associated bounds can be adjusted. By selecting the check mark to their right and entering differing values for their lower and upper bounds, the parameters can be activated for optimization. The Q-Law parameters have a special role because their choice determines not only the weighting of the individual Keplerian elements in the control law, but also whether certain elements are targeted at all or remain free. More specifically, semi-major axis, eccentricity, and inclination are always targeted, while RAAN  $\Omega$  and argument of periapsis  $\omega$  will only be considered, if their respective weights are activated in the GUI. Two examples for the set-up of the *Trajectory Arc Orbits* tab are shown in Figure 4-3.

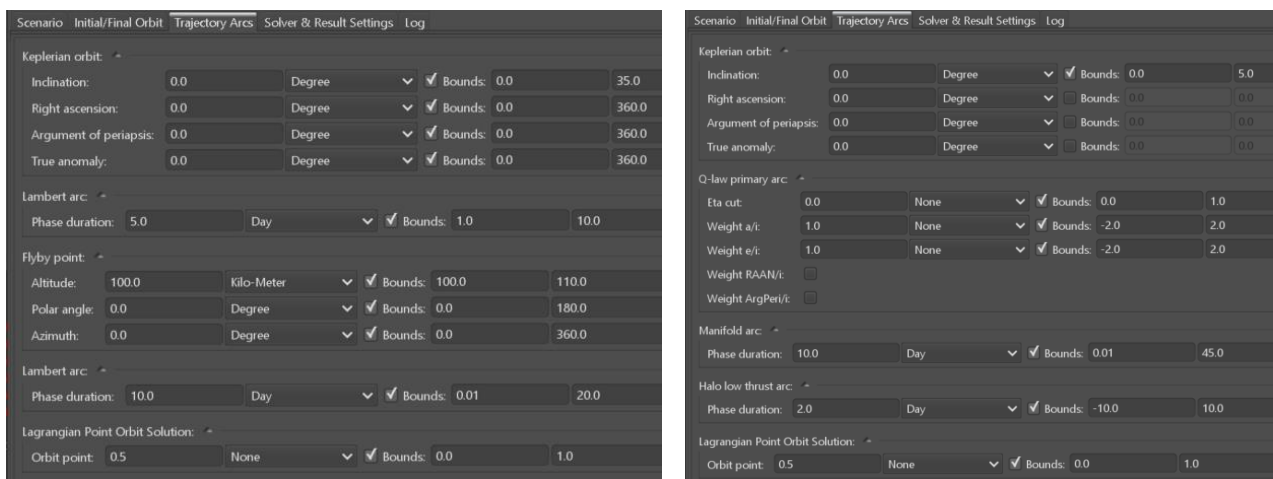


Figure 4-3: Phase Settings for (a) Fly-By Transfer

(b) Low-Thrust Transfer

### 4.4 Solver and Result Settings

In the final tab, the solver and results settings are configured. Generally, all settings here are associated with the behavior of the solver, which is used for optimizing the parameters defined in

the previous section – the MIDACO solver. It will be introduced in greater detail in chapter 5.

First, a set of stopping criteria can be defined, through which the user can determine how long the optimization process shall last at maximum or when it is considered converged. This is done through three parameters which are equivalent to MIDACO's *ALGOSTOP*, *MAXTIME* and *EVALSTOP* (see [23]). Furthermore, the definition of a seed for the solver's internal pseudo random number generator, allows for different, but reproducible optimization runs. The focus parameter allows to concentrate the solver's efforts around the current best solution and therefore attempt to improve it locally. For the initial survey of the parameter space, it is however recommended to select a small value for the focus. In order to use MIDACO's multi-objective optimization feature, the field *Create pareto front* must be set to *Enabled*. The tool will then store all solutions with Pareto-optimal trade-offs of flight duration and required  $\Delta v$ /propellant mass in a file in the specified output folder. For future versions of the Orbit Generator Tool, it is envisioned to enable the display of the Pareto front and selection of a solution directly in the GUI. If, however, only a single-objective minimization of required  $\Delta v$ /propellant mass is desired, the Pareto front field can be left disabled. The Orbit Generator will then only try to improve this characteristic and will, if necessary, spend a longer flight time to achieve this goal. Experience has shown, that often the TOF will tend towards its upper limit for single-objective simulations. Two examples are shown in Figure 4-4.

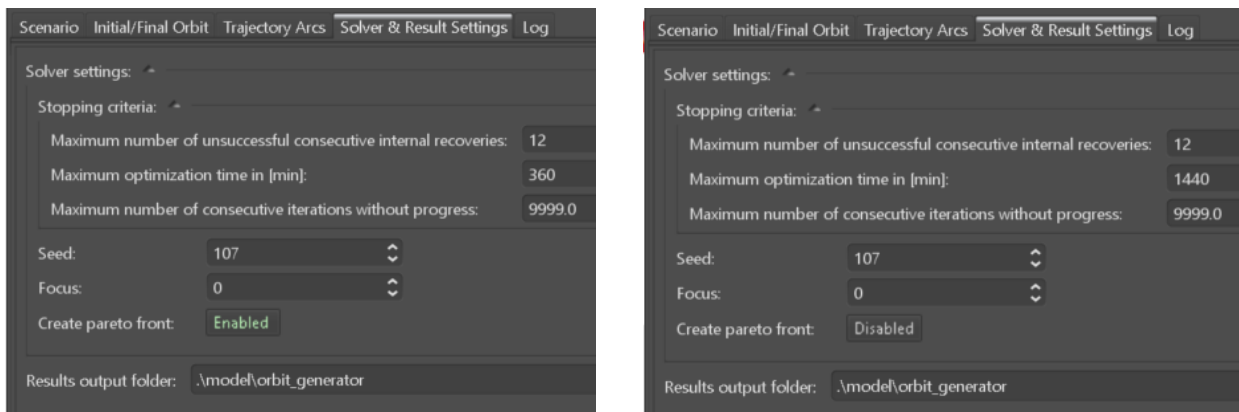


Figure 4-4: Solver Settings for (a) Multi-Objective Optimization (b) Single-Objective Optimization

## 4.5 Execution

The Orbit Generator works either in simulation or optimization mode. With *Simulate* no optimization will be performed. Only the initial values entered in the *Trajectory Arcs* tab will be used for the computation of a single transfer. This is useful especially if the user is confident in the parameter values (e.g., if they have been optimized before). The tool will save a text file containing the data of the entire transfer into the specified folder. Using *Optimize*, the solver is started and begins to optimize the transfers until it reaches one of the stopping criteria or the *Stop* button is pressed. This ends the optimization process without losing any of the data. After a simulation or a single-objective optimization, the obtained solution can be transferred into an ASTOS scenario by pressing *Apply Result*. This will activate a specially developed wizard, to carry all the settings into the scenario and include the transfer trajectory from the Orbit Generator Tool.

## 4.6 Log Output

During the simulation or optimization, the progress and transfer performance can be monitored in the log tab of the Orbit Generator GUI. The log prints and refreshes the output from MIDACO's screen-file [23]. Additionally, any problems or errors will be specified here.

## 5 PARAMETER OPTIMIZATION

A global optimization approach is used for the optimization of the trajectory arc parameters to obtain (Pareto-)optimal transfer trajectories in the CR3BP and is realized by MIDACO. MIDACO, which stands for *Mixed Integer Distributed Ant Colony Optimization*, uses an evolutionary hybrid algorithm and was developed and extended in collaboration with the European Space Agency (ESA) and the Japanese Space Exploration Agency (JAXA). Its proficiency in optimizing space transfers has been demonstrated by its developer Martin Schlueter on several occasions [24, 25]. The solver offers single- und multi-objective optimization, while being able to handle a large number of variables, constraints and objectives.

In the context of the Orbit Generator Tool, it is used to optimize the parameters associated with each of the transfer phases. In doing so, its multi-objective capability can be exploited to explore the trade-off of fast and propellant-efficient transfers. MIDACO stores the front of so-called Pareto-optimal solutions, i.e., those solutions that are not dominated by any other solution found. This concept is visualized in Figure 5-1. The Pareto-optimal solutions are made available in a text file, which allows the user to directly obtain detailed information about objective values, constraint compliance and values for the design parameters of any Pareto optimal solution. Crucially, this also enables them to reproduce any of those transfers.

The MIDACO optimizer has a multitude of configuration parameters which influence its behavior. The experience gained during the development and use of the Orbit Generator Tool has shown that it is often advantageous to perform several shorter optimizations with different values for the seed parameter. This allows a better exploration of the trade-off between TOF and  $\Delta v$ . Afterwards, a refinement of the solution of highest interest can be done by increasing the focus value.

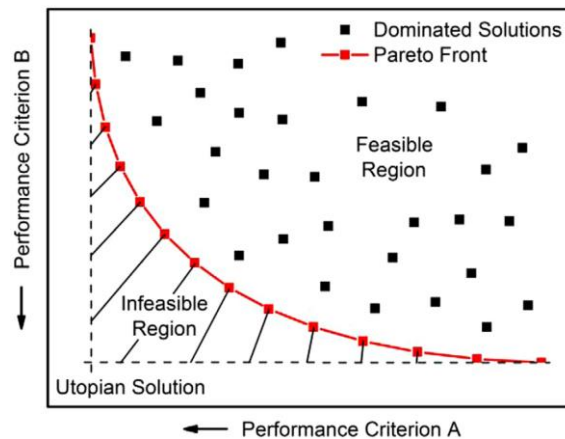


Figure 5-1: Pareto Front of a System with Two Competing Objectives [26]

## 6 RESULTS

To demonstrate the Orbit Generator Tool's capabilities and compare its performance with transfers described in literature, the following chapter will present two exemplary optimization results.

### 6.1 Scenario 1: Low-Thrust Transfer from GTO to $L_1$ Halo Orbit

The first optimization scenario is a low-thrust transfer from a geostationary transfer orbit (GTO) into a halo orbit with a z-amplitude of 8000 km around  $L_1$ . The set-up of the case, parameter bounds of each phase, and optimizer settings can be seen in Figure 4-1 (b) through Figure 4-4 (b). In order to match reference transfers from literature [27, 28, 29], a maximum transfer duration of 90 minutes was defined. Then, by leaving the Pareto front option disabled, a single-objective optimization was

executed to minimize the required propellant mass.

Table 2: Comparison of Optimized GTO to  $L_1$  Halo Transfer with Literature

	Low-Thrust Phase TOF	Manifold Phase TOF	Perturbation TOF	Total TOF	Propellant Mass Fraction
Martin et al. [27]	47.1 days	41.95 days	0 days	89.05 days	9.68%
Mingotti et al. [28]	N/A	N/A	0 days	91.5 days	8.92%
Jagannatha et al. [29]	76.34 days	13.65 days	0 days	89.99 days	8.35%
<b>This work</b>	<b>84.457 days</b>	<b>5.326 days</b>	<b>0.202 days</b>	<b>89.985 days</b>	<b>7.99%</b>

The result and a comparison with literature transfers can be seen in Table 2. After an optimization duration of 3.75 hours<sup>2</sup>, the result found by the Orbit Generator Tool had already outperformed the reference solutions with a propellant mass of 90.1 kg ( $\cong$  8.27%). As the optimization was kept running overnight, the solution was refined in the following hours and finally reached a propellant mass of 86.85 kg ( $\cong$  7.99%) after 6.8 hours. The parameters which achieved this optimal solution and the associated trajectory are depicted in Figure 6-1.

```

Scenario Initial/Final Orbit Trajectory Arcs Solver & Result Settings Log
15:00:24.3 ** RESULT *****
15:00:24.3 Total TOF (days) 89.98456957431661
15:00:24.3 Low Thrust Propellant Mass (kg) 86.8529543977811
15:00:24.3 *** Optimal Parameters ***
15:00:24.3 0 arc1.inclination 5.0
15:00:24.3 1 arc1.raan 0.0
15:00:24.3 2 arc1.omega 0.0
15:00:24.3 3 arc1.trueAnomaly 0.0
15:00:24.3 4 arc2.EtaCut 0.279438069392149
15:00:24.3 5 arc2.Weight_a_i 1.026400239388269
15:00:24.3 6 arc2.Weight_e_i 0.688021875632775
15:00:24.3 7 arc2.Weight_om_i -Infinity
15:00:24.3 8 arc2.Weight_w_i -Infinity
15:00:24.3 9 arc3.duration 5.325786675700591
15:00:24.3 10 arc3.perturbation 0.0
15:00:24.3 11 arc3.perturbationVx 0.0
15:00:24.3 12 arc3.perturbationVy 0.0
15:00:24.3 13 arc3.perturbationVz 0.0
15:00:24.3 14 arc4.duration 0.202111579152911
15:00:24.3 15 arc5.orbitPoint 0.509787741785254

```

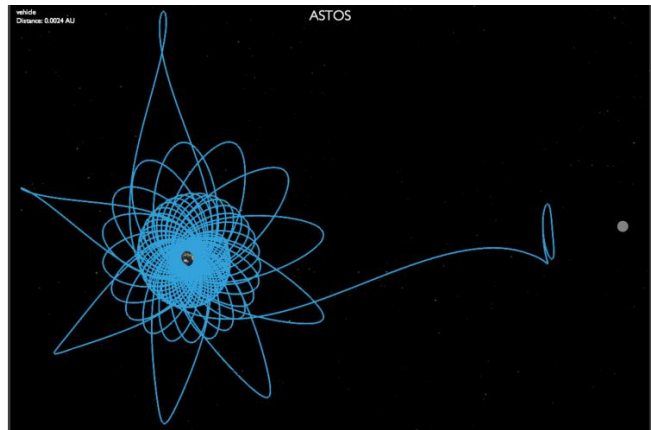


Figure 6-1: (a) Optimized Parameter Values

(b) Transfer Trajectory in Rotating CR3BP Frame

## 6.2 Scenario 2: Impulsive Transfer from LEO to $L_2$ Halo Orbit

Next, the optimization results of an impulsive lunar fly-by transfer from low Earth orbit (LEO) to a southern halo orbit around the  $L_2$  point with z-amplitude of 2000 km are presented hereinafter.

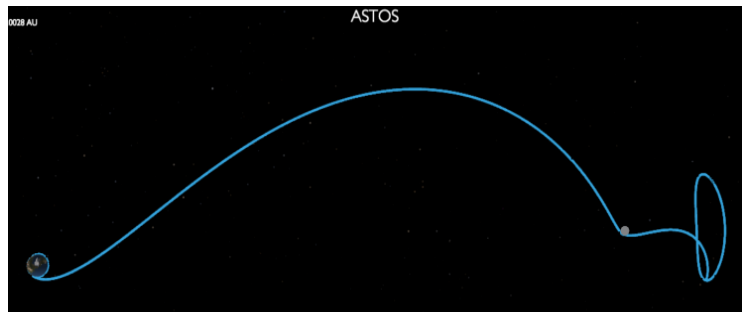
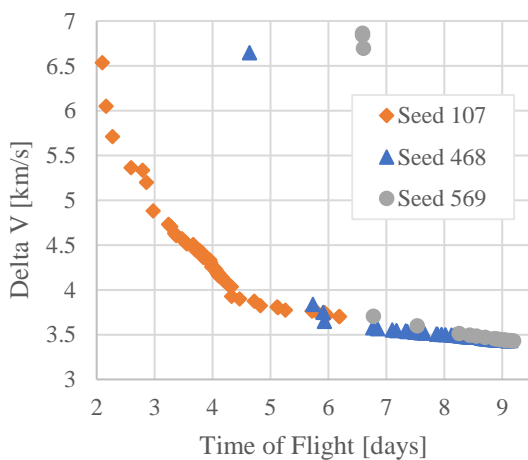


Figure 6-2: (a) Pareto Fronts

(b) Transfer Trajectory with Lowest  $\Delta v$  in CR3BP Frame

<sup>2</sup> Using MIDACO's serial optimization mode on the AMD Ryzen 7 PRO 1700X Processor with 3400 MHz.

The setup of the case can be seen in Figure 4-1 (a) to Figure 4-4 (a). As suggested earlier, instead of one long optimization run, several shorter runs of 6 hours duration were performed with different seed values. At the end of the first run, the next one was then initialized with the values of the lowest  $\Delta v$  transfer found, a different seed, and the focus value was increased from 0 to 1000 to nudge the solver to explore the trade-off towards lower  $\Delta V$  solutions. For the next optimization, the seed was changed, and the so-far best solution taken as initial guess again, while the focus value was kept at 1000. No improvement was found, and the process hence not iterated furthermore. The combination of obtained Pareto fronts and a selected transfer trajectory are depicted in Figure 6-2.

When comparing the obtained Pareto front to selected solutions from literature [13, 30, 31] in Table 3 it should be noted that they do not all target the same halo orbit. Although this deviation can make a difference for the transfer performance, the results normally differ by less than 5% [14]. It can be seen that the transfers from the Orbit Generator Tool are rather fast when compared to literature results, which results in slightly higher  $\Delta v$ . Furthermore, as the gravitational influence of the Sun is not considered, the use of low-energy transfer dynamics like the weak-stability boundary (WSB), as has been done in [13], is not yet included. However, this feature is currently under development (see also the outlook in chapter 7). Still, besides the competitive, fast transfers, the Orbit Generator Tool offers especially the advantage of a choice from several feasible solutions to mission designers.

Table 3: Literature Results for LEO to Earth-Moon  $L_2$  Halo Transfers

Reference	$\Delta V$ [km/s]	TOF [days]
Mingtao et al. [30]	Direct 3.6 - 3.7	3 - 15
	Fly-By: 3.32 - 3.4	20 - 24
	WSB: 3.19 - 3.23	80 - 120
Zazzera et al. [13]	Indirect: 3.12	77.4
	3.20	42.8
Le Bihan et al. [31]	WSB: 3.21	35
<b>This work</b>	<b>Fly-By: e.g. 3.43</b> <b>3.57</b>	<b>9.15</b> <b>6.84</b>

## 7 CONCLUSION AND OUTLOOK

The Orbit Generator Tool offers the possibility of flexibly and rapidly creating transfer trajectories in the Earth-Moon CR3BP. Using the built-in MIDACO solver, a variety of quasi-optimal transfers with different performance characteristics can be produced and their trade-off of propellant efficiency and transfer duration can be explored. Different types of orbits, such as Keplerian, halo, or distant retrograde orbits may be targeted using either impulsive or low-thrust propulsion. In doing so, the special properties of the dynamic system (in the form of fly-bys or invariant manifolds) can be deliberately exploited.

The results which can be achieved with the tool, are competitive in comparison with transfers presented in literature. Especially for low-thrust transfers or fast, impulsive transfers the produced trajectories even outperform the references under consideration. Thus, the Orbit Generator Tool can serve as an important resource for mission analysts in the early process of designing a space mission in cislunar space. The intuitive operation of the tool via the GUI furthermore simplifies the workflow.

The trajectories generated with the tool, are exported in text files and can also be simply imported into an ASTOS scenario. They serve as initial guesses for subsequent optimization, mission analysis or GNC development, also with high-fidelity ephemerides, ending up in a full featured Functional Engineering Simulator. For this purpose, a robust transformation of a CR3BP transfer into a high-fidelity trajectory is currently being developed by Astos Solutions. While more

simple transfers can be transformed to a high-fidelity ephemeris model using a direct collocation approach, this is not yet guaranteed for complex transfers.

Furthermore, to also enable low-energy transfers which utilize the Sun's gravitational influence, future releases of the Orbit Generator Tool will contain the computation of transfers in the four-body problem (4BP). Preliminary progress in implementing this system has shown that WSB transfers can be calculated with a  $\Delta v$  of 3.38 km/s at a TOF of 84 days, which is competitive with the above references in terms of performance, although there is still room for improvement. Also, the extension to the 4BP will then enable transfers between Earth-Moon and Sun-Earth halo orbits with  $\Delta v$  requirements of just a few hundreds of meters per second [32].

## 8 REFERENCES

- [1] NASA, "The Moon," NASA Space Science Data Coordinated Archive, [Online]. Available: <https://nssdc.gsfc.nasa.gov/planetary/planets/moonpage.html>. [Accessed 04 05 2023].
- [2] Y. Gao, J. Chen, B. Xu and J. Zhou, "Research on the Effectiveness of Different Estimation Algorithm on the Autonomous Orbit Determination of Lagrangian Navigation Constellation," *International Journal of Aerospace Engineering*, pp. 1-8, 2016.
- [3] Y. Ulybyshev, "Stationkeeping Strategy and Possible Lunar Halo Orbits for Long-Term Space Station," *AIAA Guidance, Navigation, and Control Conference*, 2014.
- [4] R. S. Park, W. M. Folkner, J. G. Williams and D. H. Boggs, "The JPL Planetary and Lunar Ephemerides DE440 and DE441," *The Astronomical Journal*, vol. 161, no. 3, p. 105, 2021.
- [5] United States Naval Observatory; Her Majesty's Nautical Almanac Office, *The Astronomical Almanac for the Year 2008*, London: The Stationary Office, 2006.
- [6] V. Szebehely, *Theory of Orbits: The Restricted Problem of Three Bodies*, New York, NY: Academic Press, 1967.
- [7] D. Davis, S. Bhatt, K. C. Howell, J.-W. Jang, R. Whitley, F. Clark, D. Guzzetti, E. Zimovan and G. Barton, "ORBIT MAINTENANCE AND NAVIGATION OF HUMAN SPACECRAFT AT CISLUNAR NEAR RECTILINEAR HALO ORBITS," *27th AAS/AIAA Space Flight Mechanics Meeting*, 2017.
- [8] R. Zhang, Y. Wang, H. Zhang and C. Zhang, "Transfers from distant retrograde orbits to low lunar orbits," *Celestial Dynamics and Dynamical Astronomy*, vol. 132, 2020.
- [9] D. L. Richardson, "Analytic construction of periodic orbits about the collinear points," *Celestial Mechanics and Dynamical Astronomy*, vol. 22, no. 3, pp. 241-253, 1980.
- [10] K. C. Howell, "Three-dimensional, periodic, 'halo' orbits," *Celestial Mechanics and Dynamical Astronomy*, vol. 32, no. 1, pp. 53-71, 1984.
- [11] B. P. McCarthy, "Characterization of Quasi-Periodic Orbits for Applications in the Sun-Earth and Earth-Moon Systems," Master's Thesis, Purdue University Graduate School, 2018.
- [12] M. Walther, "Definition and Optimization of Cislunar Low-Thrust Transfers," Master's Thesis, Institute of Space Systems, University of Stuttgart, 2022.
- [13] F. Bernelli Zazzera, F. Topputo and M. Massari, "Assessment of Mission Design Including Utilization of Libration Points and Weak Stability Boundaries," Advanced Concepts Team (ESTEC), 2005.
- [14] J. Tatay-Sanguesa, "Optimal Trajectories in the Earth-Moon CR3BP system," Master's Thesis, Delft University of Technology, 2021.

- [15] J. Tatay-Sanguesa, A. Wiegand and R. Noomen, "Robust Multi-Objective Trajectory Optimization Tool in the CR3BP," *8th International Conference on Astrodynamics Tools and Techniques (ICATT)*, 2021.
- [16] W. S. Koon, M. W. Lo, J. E. Marsden and S. D. Ross, "THE GENESIS TRAJECTORY AND HETEROCLINIC CONNECTIONS," *AAS/AIAA Astrodynamics Specialist Conference*, 1999.
- [17] A. E. Petropoulos, "Simple Control Laws for Low-Thrust Orbit Transfers," *AAS/AIAA Astrodynamics Specialists Conference*, 2003.
- [18] A. E. Petropoulos, "Low-Thrust Orbit Transfers Using Candidate Lyapunov Functions with a Mechanism for Coasting," *AAS Astrodynamics Specialists Conference and Exhibit*, 2004.
- [19] A. E. Petropoulos, "Refinements to the Q-law for low-thrust orbit transfers," *15th AAS/AIAA Space Flight Mechanics Conference*, 2005.
- [20] D. A. Vallado, *Fundamentals of Astrodynamics and Applications*, Microcosm Press; Springer, 2007.
- [21] J. L. Shannon, M. Ozimek, J. Atchinson and C. Hartzell, "Rapid Design and Exploration of High-Fidelity Low-Thrust Transfers to the Moon," *IEEE Aerospace Conference*, 2020.
- [22] D. Lantukh and P. Edelman, "Enhanced Q-Law Lyapunov Control for Low-Thrust Transfer and Rendezvous Design," *AAS/AIAA Astrodynamics Specialist Conference*, 2017.
- [23] MIDACO-SOLVER, "User Manual," April 2018. [Online]. Available: [http://www.midaco-solver.com/data/other/MIDACO\\_User\\_Manual.pdf](http://www.midaco-solver.com/data/other/MIDACO_User_Manual.pdf). [Accessed 16 05 2023].
- [24] M. Schlueter, "Nonlinear Mixed Integer Based Optimization Technique for Space Applications," Dissertation Thesis, Schhol of Mathematics, The University of Birmingham, 2012.
- [25] M. Schlueter, "MIDACO Software Performance on Interplanetary Trajectory Benchmarks," *Advances in Space Research (Elsevier)*, vol. 54, no. 4, pp. 744-754, 2014.
- [26] A. M. Schweidtmann, A. D. Clayton, N. Holmes, E. Bradford, R. A. Bourne and A. A. Lapkin, "Machine learning meets continuous flow chemistry: Automated optimization towards the Pareto front of multiple objectives," *Chemical Engineering Journal*, no. 352, pp. 277-282, 2018.
- [27] C. Martin and B. A. Conway, "Optimal Low-Thrust Trajectories Using Stable Manifolds," in *Spacecraft Trajectory Optimization*, Cambridge University Press, 2010, p. 238–262.
- [28] G. Mingotti, F. Topputo and F. Bernelli-Zazzera, "Combined Optimal Low-Thrust and Stable-Manifold Trajectories to the Earth-Moon Halo Orbits," *AIP Conference Proceedings*, pp. 100-112, 2007.
- [29] B. B. Jagannatha, J.-B. H. Bouvier and K. Ho, "Preliminary Design of Low-Energy, Low-Thrust Transfers to Halo Orbits Using Feedback Control," *Journal of Guidance, Control, and Dynamics*, vol. 42, no. 2, pp. 260-271, 2019.
- [30] L. Mingtao and Z. Jianhua, "Impulsive lunar Halo transfers using the stable manifolds and lunar flybys," *Acta Astronautica*, vol. 66, no. 9-10, pp. 1481-1492, 2010.
- [31] B. Le Bihan, P. Kokou and S. Lizy-Destrez, "Computing an optimized trajectory between Earth and an EML2 halo orbit," *AIAA Guidance, Navigation, and Control Conference*, 2014.
- [32] A. Maisch, "Design of Trajectories between Lagrangian Orbits in the 4-Body Problem," Master's Thesis, Astos Solutions GmbH; Institute of Space Systems, University of Stuttgart, 2022.